June 2023

Fondazione Eni Enrico Mattei

Working Paper

011.2023

The connectedness of Energy Transition Metals

Andrea Bastianin, Chiara Casoli, Marzio Galeotti

The connectedness of Energy Transition Metals

By **Andrea Bastianin** (Department of Economics, Management, and Quantitative Methods, University of Milan and Fondazione Eni Enrico Mattei)
Chiara Casoli (Fondazione Eni Enrico Mattei)
Marzio Galeotti (Department of Environmental Science and Policy, University of Milan and Fondazione Eni Enrico Mattei)

Summary

We assess the degree of connectedness among 16 metals that are critical for the production of clean energy technologies. These commodities are the constituents of the Energy Transition Metals (ETMs) price index maintained by the International Monetary Fund and comprise base, precious, and minor metals. We rely on Vector Autoregressive models and generalized forecast error variance decomposition to quantify spillovers among ETMs returns and volatilities. By calculating both static and dynamic measures of connectedness, we gain insight into the patterns of shock transmission between ETMs. Our static analysis reveals that base and precious metals are net shock transmitters, while minor and most battery metals are net receivers. By splitting the analysis into three groups, we find that almost half of the connectedness originates within each group, whereas the other half is due to cross-group spillovers. Moreover, we find that the system-wide connectedness of returns is positively correlated with proxies of economic activity, whereas volatility connectedness seems to be more related to global economic policy uncertainty.

JEL Classification: C32; Q02; Q41; Q43; Q48

Keywords: Connectedness; Energy Transition; Metals; Raw materials

***Address for correspondence*:**
Chiara Casoli
Researcher, *Econometrics of the Energy Transition (EET) Program*
Fondazione Eni Enrico Mattei, Corso Magenta 63, 20123 Milan (Italy)
email: chiara.casoli@feem.it

The connectedness of Energy Transition Metals

Andrea Bastianin[a,c] Chiara Casoli[c,*] Marzio Galeotti[b,c]

June 26, 2023

Abstract: We assess the degree of connectedness among 16 metals that are critical for the production of clean energy technologies. These commodities are the constituents of the Energy Transition Metals (ETMs) price index maintained by the International Monetary Fund and comprise base, precious, and minor metals. We rely on Vector Autoregressive models and generalized forecast error variance decomposition to quantify spillovers among ETMs returns and volatilities. By calculating both static and dynamic measures of connectedness, we gain insight into the patterns of shock transmission between ETMs. Our static analysis reveals that base and precious metals are net shock transmitters, while minor and most battery metals are net receivers. By splitting the analysis into three groups, we find that almost half of the connectedness originates within each group, whereas the other half is due to cross-group spillovers. Moreover, we find that the system-wide connectedness of returns is positively correlated with proxies of economic activity, whereas volatility connectedness seems to be more related to global economic policy uncertainty.

Key Words: Connectedness; Energy Transition; Metals; Raw materials.

JEL Codes: C32; Q02; Q41; Q43; Q48.

[(a)] Department of Economics, Management, and Quantitative Methods, University of Milan, Milan, Italy.

[(b)] Department of Environmental Science and Policy, University of Milan, Milan, Italy.

[(c)] Fondazione Eni Enrico Mattei, Milan, Italy.

[(*)] *Corresponding author*: Chiara Casoli, Fondazione Eni Enrico Mattei, Corso Magenta, 63, 20123, Milan, Italy. Email: chiara.casoli@feem.it.

Acknowledgements: we thank for their comments participants to the to the 9th International Symposium on Environment and Energy Finance Issues held in Paris in May 2023.

1 Introduction

There is by now broad consensus on the need to drastically reduce emissions of greenhouse gases worldwide if we are to limit the temperature increase to 1.5-2°C relative to pre-industrial levels and thus prevent the major damages from climate change. Awareness of these risks has stimulated a process of radical change of energy systems and of decarbonisation of economies more generally.

The global energy transition (ET) is now well under way and has recently focused on the goal of reaching net zero emissions (NZE) by mid-century. The alternative pathways to NZE that several institutions have analysed share a common trait: the complexity of the transition. Decarbonisation entails increasing penetration of renewable energy technologies especially in power generation, electrification of entire sectors of the economy such as transport, diffusion of more energy efficient devices, instruments, appliances, and consumer goods, increasing use of hydrogen.

Besides the clear environmental benefits, it has been claimed that the ET will also create jobs and stimulate economic growth. The downside is that a host of critical minerals and metals are required for green energy technologies. For example, solar photovoltaic panels use silicon, tellurium, gallium, and indium; fuel cells use elements from the platinum group; batteries for electric vehicles and energy storage use lithium and cobalt; wind turbines and electric vehicles use dysprosium, terbium, europium, neodymium, and yttrium. Lists of CRMs are compiled and regularly updated by many governmental agencies (European Commission, 2020b; Nakano, 2021; U.S. Department of the Interior, 2022). On 16 March 2023 the European Commission presented a Proposal for a *Regulation establishing a framework for ensuring a secure and sustainable supply of critical raw materials* known as "European Critical Raw Materials Act".[1]

Critical raw materials (CRMs) are increasingly relevant in several technological domains and having access to them might soon become as essential as having access to reliable energy supplies. While phasing out fossils fuels, countries engaged in the ET have to phase in critical materials. Broadly speaking, CRMs are economically and strategically important inputs

[1] See `https://ec.europa.eu/commission/presscorner/detail/en/ip_23_1661`.

characterised by a low degree of substitutability and a high-supply risk. As an advanced country that is ahead in the race toward NZE, the EU is largely "materials-dependent". This follows from the fact that the ET is materials-intensive and the supply of CRMs is largely controlled by a limited number of countries. Scarcity of these CRMs might hamper the large-scale deployment of technologies in strategic sectors such as renewable energy, e-mobility, defence and aerospace (European Commission, 2020a).

In this paper we focus on a subset of raw materials, which we call Energy Transition Metals (ETMs), that are input in the production of clean energy technologies such as solar, wind, batteries and fuel cells. Borrowing from the burgeoning literature on energy security, we can conceptualize ETMs security focusing on four dimensions: availability, affordability, efficiency, and environmental stewardship (Metcalf, 2014; Sovacool and Brown, 2010). While ETMs exhibit criticalities related to all of such dimensions, we mainly focus on the interplay between availability and affordability.[2]

In terms of availability, defined as the ability to procure a sufficient, safe and diversified supply of ETMs, the production of most of the metals considered in this study is highly concentrated geographically, often in poor or developing countries. This makes materials-dependent countries prone to supply shocks, just like oil-dependent economies. As a matter of fact, in the words of the European Commission President Ursula von der Leyen "*lithium and rare earths will soon be more important than oil and gas*".[3]

Affordability relates, among other things, to the provision of ETMs at stable prices (Yergin, 2006). As shown in Figure 1, the prices of ETMs are highly volatile. Since the mid-70s the energy economic literature has devoted renewed attention to the impact of oil shocks on energy-dependent economies (Bastianin et al., 2017; Hamilton, 2009; Kilian, 2008, 2009; Peersman and Van Robays, 2012) as well as on oil-rich economies (Ahmadi and Manera, 2021; Berument et al., 2010; Esfahani et al., 2014). The methodologies and results of that literature contain important insights for the affordability of ETMs.

Availability and affordability factors are intertwined and both help explain a large portion of the volatility observed in the prices of ETMs. In fact, the combination of low

[2] See Lèbre et al. (2020); Owen et al. (2022); Zhang et al. (2022) for a broader perspective.

[3] See: `https://ec.europa.eu/commission/presscorner/detail/en/STATEMENT_22_5523`.

substitutability, low price elasticity of supply and demand and a high concentration of production in few countries implies that even small shocks arising on either side of the markets for ETMs can trigger large price responses (Boer et al., 2021; Fally and Sayre, 2018; Graedel et al., 2015a,b).

The existence of liquid futures markets – performing their functions of price discovery and risk mitigation – for ETMs could in principle contribute to ETM security by improving their affordability for different classes of stakeholders, including firms along the supply chain of technologies necessary for the ET. However, while for some of the ETMs in our sample derivative markets are liquid and have a long history (e.g. many base and precious metals), most of the metals that are in high demand for clean energy technologies, such as cobalt or rare earth elements, do not have well developed futures markets.

The oil and gas dependence that characterises several countries presents many analogies with the potential materials dependence those countries might soon experience. There are also important differences, one of which is the fact that while there is only "one" oil – and only "one" gas – there are many ETMs and they are largely intertwined as subsets of them are mined together, they are jointly processed and are often complementary, or low substitutable, inputs. As a consequence, ETMs have to be considered in a "connected" way.

In this paper we assess the degree of spillovers or connectedness among 16 ETMs that are critical for the production of clean energy technologies and are the constituents of the Energy Transition Metals (ETMs) price index maintained by the International Monetary Fund (IMF). By calculating both static and dynamic measures of connectedness for commodity returns and volatilities, we can gain insight into the patterns of shock transmission within the ETMs. In this paper we follow the methodology put forth by Diebold and Yilmaz (2009, 2012, 2014) and rely on a Generalised Forecast Error Variance Decomposition (GFEVD) from Vector Autoregressive (VAR) models to construct measures of directional spillovers among ETMs.

Alternatives ways to measure connectedness have been proposed in the literature. These include principal components analysis and Granger-causality (Billio et al., 2012) and the approach based on network analysis techniques for time-series (Barigozzi and Brownlees, 2019; Barigozzi et al., 2022). Moreover, other methods focus on the asymmetry of connectedness at different frequencies or quantiles of the distribution (Baruník and Kley, 2019; Baruník and Křehlík, 2018; Zhu et al., 2019).

GFEVD-based connectedness is probably the most widely used approach and has the advantage of measuring spillover from each commodity to others without identification assumptions or imposing a particular ordering of the endogenous variables in the VAR (Koop et al., 1996; Pesaran and Shin, 1998). Moreover, Diebold and Yilmaz (2014) highlight the close relationship between connectedness measures based on GFEVD and key statistics used in the field of network analysis. Estimating network effects is crucial because it is well recognised that sectoral microeconomic shocks can propagate and eventually result in aggregate fluctuations (Acemoglu et al., 2012) and contagion from a large number of entities or markets may result in systemic crises (Bandt et al., 2012). Additionally, ETM price shocks, like any other commodity price shock, are important in that they can affect commodity supply, may weaken the financial sector and price stability and eventually result in a deterioration of the terms of trade for commodity exporter economies (Garcia and González, 2013; Kilian, 2009; Kinda et al., 2018; Sekine and Tsuruga, 2018).

An application of the GFEVD-based methodology to commodity connectedness, focusing on volatility spillovers, is provided by Diebold et al. (2018). Recent surveys of the literature dealing with this methodology are provided by Balcilar et al. (2022); Diebold and Yilmaz (2023). As far as we know this paper is the first to focus on the connectedness of a large set of ETMs. Measuring ETM connectdness is central for risk measurement and management both from the perspective of private sector investment (e.g. for producers of clean energy technologies) and for the formulation of public policies (e.g. connectedness tends to increase during commodity-market crises).

The rest of the paper is organized as follows. Section 2 describes data and econometrics methods underlying our analysis; Section 3 presents our main results while Section 4 concludes. An Appendix with further details and results completes the paper.

2 Data and methods

2.1 Data

We analyse 16 ETMs, comprised of 7 base metals (aluminum, cobalt, copper, lead, molybdenum, nickel, zinc), 3 precious metals (palladium, platinum, silver) and 6 minor metals (chromium, lithium, manganese, rare earth elements, silicon, vanadium) that we will define generically as "other ETMs". These metals are the constituents of the IMF's ETMs price index.[4] This index and the prices of its constituents are available at monthly sampling frequency and therefore are not suitable for our analysis that requires returns and realised volatility (RV) measures. To build such measures, we recover daily prices of the constituents of the IMF's ETMs price index from Refinitiv Eikon.

Table 1 shows the list of commodities and the clean energy technologies for which they are used. This table also reports the weight of each commodity in IMF's ETMs price index that is based on the share of imports of each metal in total world commodity imports. As we can see, traditional base metals – such as aluminium and copper – with a wide range of industrial uses get most of the weight in the IMF index. On the contrary, cobalt, rare earth elements (REE), lithium and other minor metals – chiefly used in clean energy technologies – represent a small share of global imports.[5] Table 1 also reveals that the production of most minor metals is highly geographically concentrated. For instance, over 60% of the world production of REE, silicon and vanadium is concentrated in China, while the Democratic Republic of Congo is the leader producer of cobalt.

Some base and precious metals in our sample have been traded in future exchanges for many years, while other minerals – notably those labelled as "other ETMs" in the second column of Table 1 – have a much shorter price history. The low liquidity of markets for these ETMs implies that their prices change infrequently and hence working with daily or weekly

[4]The ETM price index is described in the "Technical Documentation" that accompanies the data avaiable on the IMF Primary Commodity Prices portal. See: `https://www.imf.org/en/Research/commodity-prices` and Table A1 in Appendix A.

[5]Some of these metals – such as cobalt, copper, nickel, lithium and manganese – are often referred to as battery metals.

Table 1: Energy Transition Metals: classification, sources and uses

Metal	Group	IMF weight %	Top Producer (% world)	Main Uses
Aluminum	Base	15.9	Australia (28)	All sectors
Cobalt	Base	0.6	Congo (DRC) (71)	Li-ion batteries. Fuel Cells
Copper	Base	34.3	Chile (26)	All sectors
Lead	Base	3.8	China (47)	Wind. PV
Molybdenum	Base	5.3	China (43)	Wind. PV
Nickel	Base	6.7	Indonesia (37)	Li-ion batteries. Fuel Cells. PV. Wind
Zinc	Base	6.1	China (32)	PV
Palladium	Precious	3.1	South Africa (40)	Fuel Cells
Platinum	Precious	4.4	South Africa (72)	Fuel Cells
Silver	Precious	7.0	Mexico (23)	Fuel Cells. PV
Chromium	Other	3.2	South Africa (44)	Fuel cells. Wind
Lithium	Other	0.3	Australia (55)	Li-ion batteries
Manganese	Other	3.7	South Africa (37)	Wind. Li-ion batteries
REE	Other	0.5	China (60)	Wind. EV
Silicon	Other	5.1	China (71)	Li-ion batteries
Vanadium	Other	0.2	China (66)	Fuel Cells

Notes: data on the leading producing countries and the relative production as a share of world total are provided by the USGS in the Mineral Commodity Summaries 2022 report. The main uses for each mineral are taken from the Critical Raw Materials for Strategic Technologies and Sectors in the EU report by the European Commission and refer to the use within the European Union. IMF weights represent the share of imports of metal m in total global commodity import and are available at `https://www.imf.org/en/Research/commodity-prices`. PV stands for photovoltaic, EV for electric vehicles.

data is unfeasible.[6]

Daily data are then aggregated to construct monthly returns and realised volatilities that span a sample running from June 2012 to December 2022, for a total of 127 observations. Denoting daily real prices for metal m as P_{m,t_d} and daily log-returns as $r_{m,t_d} = 100 \times \log(P_{m,t_d}/P_{m,t_d-1})$, we compute monthly RV as follows:[7]

$$RV_{m,t} = \frac{1}{D_t} \sum_{t_d=1}^{D_t} r^2_{m,t_d},$$

where D_t is the number of days in month t. In subsequent analyses we rely on monthly real returns $r_{m,t} = (1/D_t) \sum_{t_d=1}^{D_t} r_{m,t_d}$ and $\log \sqrt{RV_{m,t}}$. We consider log of realised standard deviations in that RV_t is extremely skewed, while $\log \sqrt{RV_{m,t}}$ is approximately Gaussian

[6] We report the percentage of zero monthly returns as a measure of illiquidity of different markets: cobalt (3.97%), molybdenum (7.95%), manganese (7.14%), silicon (38.10%), vanadium (37.30%).

[7] Daily prices are deflated using the interpolated Consumer Price Index for the US.

for most commodities (see Andersen et al., 2001; French et al., 1987, for a discussion in the context of stock market volatilities). For simplicity, from now on we keep on using the shorthand notation RV, even though we rely on log $\sqrt{RV_{m,t}}$ in the analyses.

Figure 1: Price of Energy Transition Metals: June 2012 - December 2022

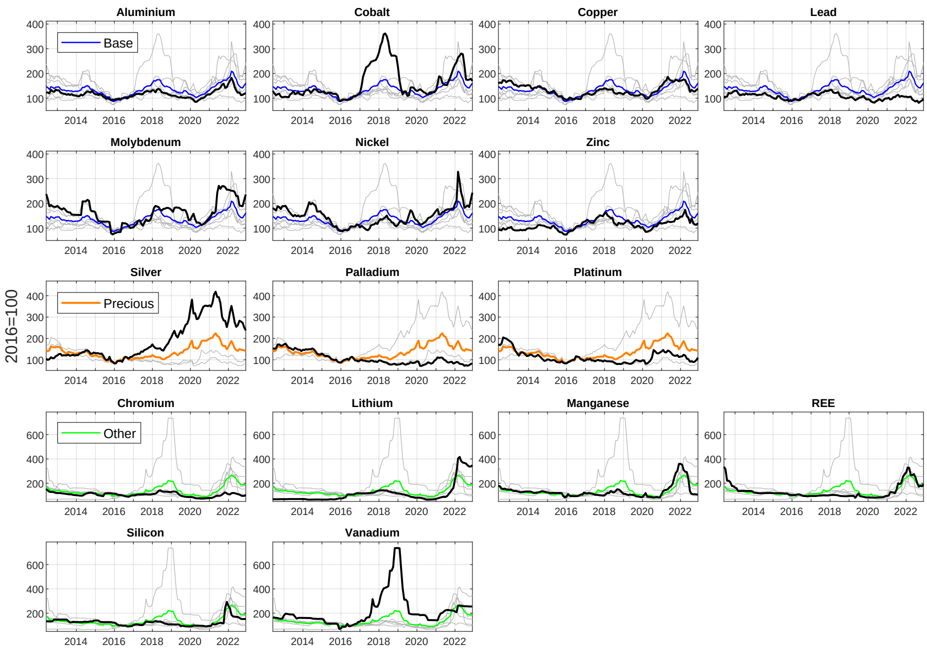

Notes: for each commodity, the figure shows its price (black line) and the price index for the category of metals (coloured line) to which it belongs. Prices have been normalised as follows: $100 \times P_{mt}/\bar{P}_m^{2016}$ where $\bar{P}_m^{2016}$ is the average price of m for 2016. Metal groups are defined in Table 1.

Figure 1 shows the real prices of ETMs in our sample. The prices of base metals, reported in first two rows of the figure, exhibit some cycles and tend to be higher at the end of the sample. Among precious metals – shown on the third row of Figure 1 – silver displays the largest surge during the second part of the sample. Finally, other ETMs prices are in general characterised by less variability, and for the majority of them there is evidence for a price increase after the COVID-19 pandemic. The only exception is vanadium price, exhibiting a remarkable spike between 2017 and 2020. Such a spectacular rise is due to a set of events affecting both the supply and demand-side of the Chinese market. First, in 2017 China enforced stricter environmental rules; as a consequence, inspections led to temporary or even permanent closing of some vanadium producers. Moreover, in 2018, China released a new standard for high-strength reinforcing bars. These were required to have a higher percentage of vanadium and hence increased overall domestic consumption of this metal. Further graphs and details about the data are reported in Appendix A.

2.2 VAR estimation

To obtain connectedness measures based on the GFEVD, the first step is to estimate VAR models for monthly returns and RVs. While we do include a constant in our specification, for ease of notation we now consider a zero-mean VAR process:

$$\mathbf{y}_t = \sum_{\ell=1}^{p} \mathbf{A}_\ell \mathbf{y}_{t-\ell} + \mathbf{u}_t, \tag{1}$$

where $\mathbf{y}_t$ is an $M \times 1$ vector with $M = 16$ and the m-th element corresponding either to r_t^m or $\log \sqrt{RV_{m,t}}$, $\mathbf{u}_t \sim (\mathbf{0}, \mathbf{\Sigma})$ and $\mathbf{A}_\ell$ is an $M \times M$ matrix of coefficients. The choice of the lag order, p, is critical in that the number of coefficients to be estimated is $M + M^2 p$ and hence grows quadratically with p.[8]

We handle dimensionality issues by estimating VAR models with an adaptive elastic-net penalty (Zou and Zhang, 2009) which involves both shrinkage and selection. The penalised estimation approach induces sparsity in the coefficient matrices $\mathbf{A}_\ell$. As noted in Nicholson et al. (2017), taking into account the sparsity patterns allows to address over-parametrisation in VAR models without having to select a low lag order p. In low-dimensional settings, the VAR model in Equation (1) is estimated via Ordinary Least Squares. However, as M and p increase, reducing the parameter space of the VAR becomes essential. The adaptive elastic-net consists of adding an appropriate penalty term to Equation (1). Specifically, fitting a sparse VAR involves solving the following penalised estimation problem:

$$\min_{\mathbf{A}} \sum_{t=1}^{T} \left|\left| \mathbf{y}_t - \sum_{\ell=1}^{p} \mathbf{A}_\ell \mathbf{y}_{t-\ell} \right|\right|_F^2 + \lambda \mathcal{P}_y(\mathbf{A}) \quad \text{for } \lambda \geq 0, \tag{2}$$

where $||\cdot||_F$ denotes the Frobenius norm and $\mathcal{P}_y(\mathbf{A})$ represents the penalty structure applied to the coefficient matrices $\mathbf{A} = [\mathbf{A}_1, \ldots, \mathbf{A}_p]$.[9] The adaptive elastic-net VAR estimator

[8]For instance, with $M = 16$, VAR(3) and VAR(4) models respectively involve estimating 784 and 1040 coefficients.

[9]The Frobenius norm of an $(Z \times K)$ matrix $\mathbf{B}$ is defined as $||\mathbf{B}||_F = \sqrt{\sum_{z=1}^{Z} \sum_{k=1}^{K} |b_{zk}|^2}$. The 1-norm

Figure 2: VAR model for returns: sparsity

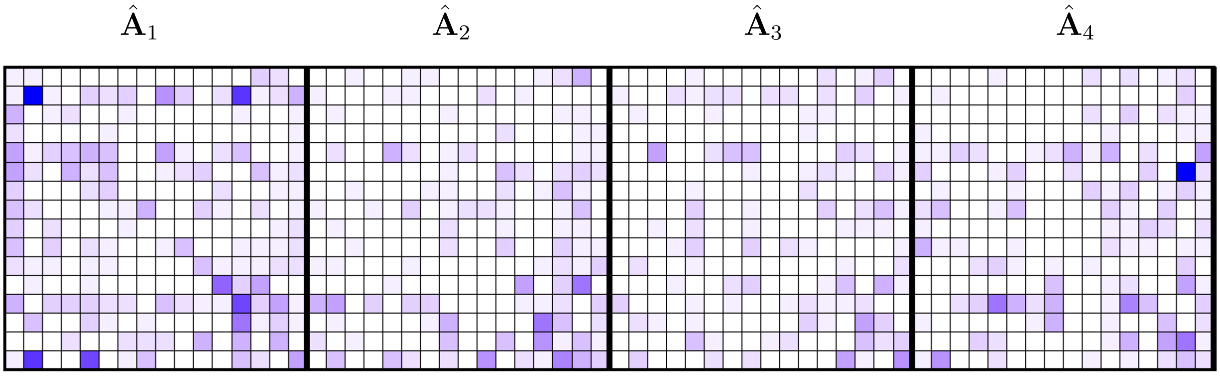

Notes: colored shades indicate active coefficients, with darker shades referring to parameters that are larger in magnitude. White areas denotes coefficients that have been set to zero.

imposes the following penalty to Equation (2):

$$\mathcal{P}_y(\mathbf{A}) = \alpha||\mathbf{A}||_1 + (1-\alpha)||\mathbf{A}||_2^2, \quad \text{for } 0 \leq \alpha \leq 1. \tag{3}$$

The parameter α measures the trade-off between LASSO and ridge penalties in Equation (3). When $\alpha = 1$, the penalty function yields the LASSO estimator (Tibshirani, 1996). On the other hand, as $\alpha \to 0$, the LASSO penalty shrinks toward 0, the elastic-net becomes closer to ridge regression (Hoerl and Kennard, 1988). The optimal penalty parameters λ and α can be determined using cross-validation, allowing for a completely data-driven approach.[10]

Figure 2 shows the sparsity pattern for the estimated matrices of coefficients in the case of a VAR(4) for returns. As we can see, elements along the main diagonal of $\hat{A}_1$ have darker shades, while off-diagonal elements are often shrunk toward zero. It is worth noting that within this framework, VAR(p) denotes a VAR with a lag order at most equal to p, and the effective lag order is determined equation by equation by the penalty function (see Nicholson et al., 2017, for further details).

is $||\mathbf{B}||_1 = \max_{1 \leq k \leq K} \sum_{z=1}^{Z} |b_{zk}|$ and the 2-norm can be written as $||\mathbf{B}||_2 = \sqrt{\lambda_{max}\mathbf{B}^*\mathbf{B}}$, where λ_{max} is the maximum eigenvalue of $\mathbf{B}^*\mathbf{B}$ and $\mathbf{B}^*$ is the conjugate transpose of $\mathbf{B}$.

[10] We set α equal to $(1+M)^{-1} \approx 0.059$. Then, the optimal $\hat{\lambda}$ is selected from a grid of values $\lambda_1, \ldots \lambda_n$ via a rolling procedure, between times $T_1 = T/3$ and $T_2 = 2T/3$. The final $\hat{\lambda}$ is the value that minimises the Mean Squared Forecast Error. The grid of values for the choice of $\hat{\lambda}$ is specified by selecting the grid depth and the number of grid values. We set for the returns analysis the grid depth at 50 and the number of values to 10, whereas for RV we opt for an increased grid depth of 500.

2.3 Measuring connectedness

Our connectedness analysis relies on the GFEVD of the VAR as proposed in a series of papers by Diebold and Yilmaz (2009, 2012, 2014). The GFEVD does not require orthogonalising shocks and is invariant to the ordering of the variables in the VAR:

$$\theta_{ij}(H) = \frac{\sigma_{jj}^{-1}\sum_{h=0}^{H-1}\left(\mathbf{e}_i'\boldsymbol{\Phi}_h\boldsymbol{\Sigma}\mathbf{e}_j\right)^2}{\sum_{h=0}^{H-1}\left(\mathbf{e}_i'\boldsymbol{\Phi}_h\boldsymbol{\Sigma}\boldsymbol{\Phi}_h'\mathbf{e}_i\right)} \quad H = 1, 2, \ldots \text{ and } i, j = 1, ..., M$$

where $\boldsymbol{\Sigma}$ is the covariance matrix of the σ_{jj} the standard deviation of the disturbance of the j-th equation, $\mathbf{e}_j$ is a selection vector with one as j-th element and zero otherwise and the matrices $\boldsymbol{\Phi}_k$ are derived from the moving average representation of the VAR model in Equation (1).[11] Since the variance shares do not sum to one (i.e. $\sum_{j=1}^{M}\theta_{ij}(H) \neq 1$), we consider the following normalization:

$$C_{i\leftarrow j}^{H} \equiv \tilde{\theta}_{ij}(H) = 100 \times \frac{\theta_{ij}(H)}{\sum_{j=1}^{M}\theta_{ij}(H)}. \tag{4}$$

The generic element $C_{i\leftarrow j}^{H} \equiv \tilde{\theta}_{ij}(H)$ is a measure of *Gross-Pairwise* directional connectedness from j to i; it measures the percentage contribution of mineral j to mineral's i generalised forecast error variance at horizon H. Note that in general $C_{i\leftarrow j}^{H} \neq C_{j\leftarrow i}^{H}$. Armed with pairwise directional connectdness measures, we can compute the following statistics (from now on we drop the H superscript for ease of notation):

$$\textit{Net-Pairwise:} \qquad C_{ij} = C_{j\leftarrow i} - C_{i\leftarrow j} \tag{5}$$

$$\textit{From:} \qquad C_{i\leftarrow\bullet} = \frac{1}{M}\sum_{\substack{j=1\\ i\neq j}}^{M}\tilde{\theta}_{ij}(H) \tag{6}$$

$$\textit{To:} \qquad C_{\bullet\leftarrow j} = \frac{1}{M}\sum_{\substack{i=1\\ i\neq j}}^{M}\tilde{\theta}_{ij}(H) \tag{7}$$

$$\textit{Net:} \qquad C_{i} = C_{\bullet\leftarrow i} - C_{i\leftarrow\bullet} \tag{8}$$

[11] A stable VAR process can be rewritten in moving average form as follows: $\mathbf{y}_t = \sum_{k=0}^{\infty}\boldsymbol{\Phi}_k\mathbf{u}_{t-k}$, where $\boldsymbol{\Phi}_0 = I_M$ and $\boldsymbol{\Phi}_k = \sum_{\ell=1}^{k}\boldsymbol{\Phi}_{k-\ell}\mathbf{A}_\ell$ for $k = 1, 2, \ldots$ and $\mathbf{A}_\ell = \mathbf{0}$ for $k > p$.

$$\textit{Total}: \qquad C = \frac{1}{M}\sum_{i=1}^{M}\sum_{\substack{j=1 \\ i\neq j}}^{M}\tilde{\theta}_{ij}(H) \tag{9}$$

Notice that *Net-Pairwise* connectedness in Equation (5) differs from *Gross-Pairwise* directional connectedness in Equation (4). First, while there are $(M^2 - M)/2$ net-pairwise connectedness measures, there are M^2 gross-pairwise connectedness measures. In our framework, gross-pairwise directional connectedness represents a measure of bilateral spillovers, whereas its "net" counterpart allows to divide minerals into net-receivers and net-transmitters of shocks. Measures in Equation (6) and (7) are often labelled respectively as *From* and *To* connectedness, since they define the transmitted and the received spillover for the i-th mineral, and correspond to the off-diagonal row and column sums of the connectedness table (CT). A sketch of the CT for our analysis is shown in Figure 3.

Total or system-wide connectedness. Connectedness simply corresponds to the sum of From – or To, equivalently – directional connectedness. Note that $\sum_{j=1}^{M} C_{\bullet\leftarrow j} = \sum_{i=1}^{M} C_{i\leftarrow\bullet} = C$. The connectedness table is a $(M+1)\times(M+1)$ matrix with $C_{i\leftarrow j}$ in the first M rows and columns. The $M+1$-th column (row) reports From (To) connectedness, while system-wide connectedness appears in the lower right corner. Diebold and Yilmaz (2014) show that the GFEVD represents the adjacency matrix of a directed weighted network.[12] Specifically, the GFEVD delivers a matrix whose entries capture the strength and direction of spillovers between commodities. Moreover, it can be shown that From, To and system-wide connectedness are equivalent to key statistics used in the network literature (e.g. in-degrees, out-degrees and mean degree).

Connectedness within and across groups. In order to capture the differential impact of different groups of commodities, the CT is aggregated into blocks that correspond to base, precious, and other metals, respectively. See Figure 3. To this end, we define a group index vector $\mathbf{G}$ of size $(M \times 1)$ that assigns each of the M commodities to a group $g = 1, 2, 3$.[13]

[12] Note that, in general, a graph or adjacency matrix $\mathcal{A}$ has elements a_{ij} that indicate edges from i to j. On the contrary, in our approach each entries of the CT measures a spillover from j to i.

[13] In our setting, the commodities are ordered according to the group they belong to, with the first 7 entries of $\mathbf{G}$ identifying base metals and being equal to one, entries 8-10 identifying precious metals and being equal to two, and the remaining 6 entries identifying other metals and being equal to three.

To compute the *within-group connectedness* of each group, we sum all the elements in the CT that pertain to that group, net of the contribution of own shocks to GFEVD:

$$C_{g\leftarrow g} = \frac{1}{M}\sum_{i=1}^{M}\sum_{\substack{j=1\\ j\neq i}}^{M} C_{i\leftarrow j}\cdot I(G_i = g)\cdot I(G_j = g) \quad g = 1, 2, 3, \tag{10}$$

where $I(G_i = g)$ is an indicator function that is equal to 1 if $G_i = g$ and 0 otherwise. Summing over g we get the *system-wise within-group connectedness*: $C_{within} = \sum_{g=1}^{3} C_{g\leftarrow g}$. *Connectedness across groups* can be defined as follows:

$$C_{k\leftarrow z} = \frac{1}{M}\sum_{i=1}^{M}\sum_{j=1}^{M} C_{i\leftarrow j}\cdot I(G_i = k)\cdot I(G_j = z) \quad k, z = 1, 2, 3 \text{ with } k \neq z. \tag{11}$$

Notice that with three groups there are 6 different cross-group connectedness measures. System-wide cross-group connectedness is equal to $C_{between} = \sum_{k=1}^{3}\sum_{\substack{z=1\\ k\neq z}}^{3} C_{k\leftarrow z}$. It follows that: $C = C_{within} + C_{between}$. The distinction between connectedness within and across groups is illustrated in Figure 3.

Figure 3: Connectedntess within and between groups

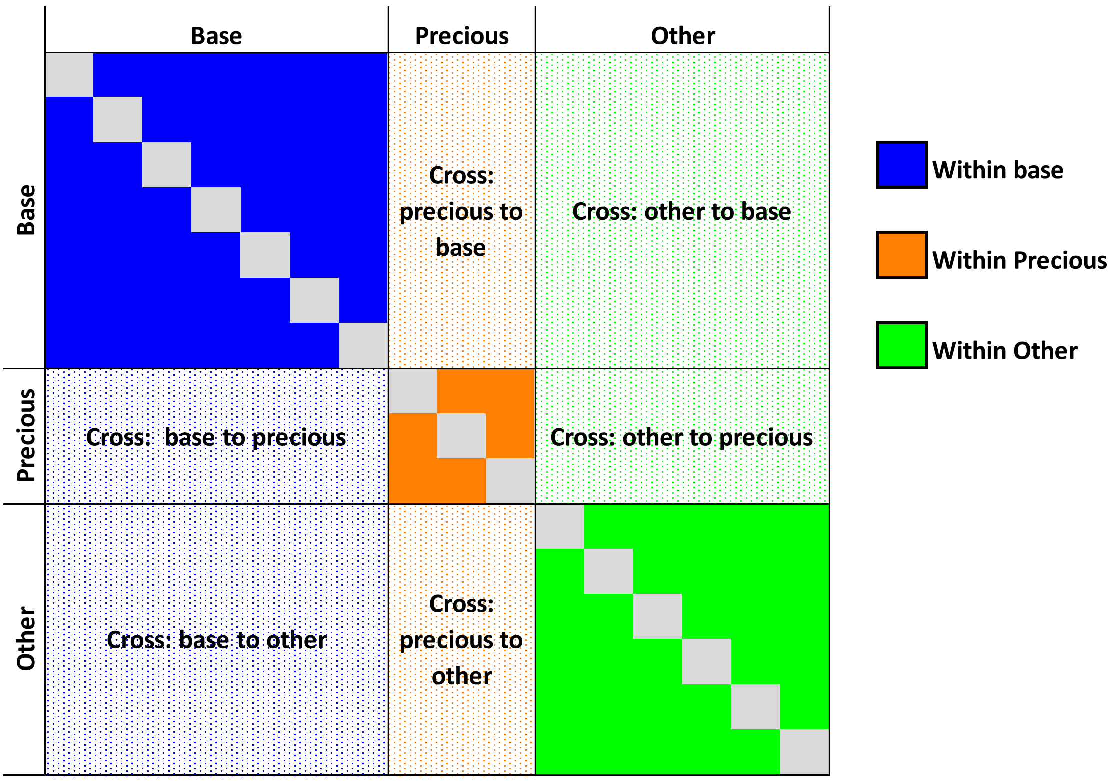

To and From group-connectedness. To connectedness for group g is simply the sum of to connectedness for metals in group g:

$$C_{\bullet \leftarrow g} = \sum_{j=1}^{M} C_{\bullet \leftarrow j} \cdot I(G_j = g). \tag{12}$$

Similarly, From connectedness for groups is:

$$C_{g \leftarrow \bullet} = \sum_{i=1}^{M} C_{i \leftarrow \bullet} \cdot I(G_i = g) \tag{13}$$

It follows that $C = \sum_{g=1}^{3} C_{\bullet \leftarrow g} = \sum_{g=1}^{3} C_{g \leftarrow \bullet}$.

3 Results

The VAR lag order, p, is equal to 4 in the case of returns, whereas we set $p = 3$ for RV. We report results based on the GFEVD at $H = 3$ months horizon.[14] Since returns and volatilities measure different economic concepts, so does connectedness among them. Connectedness for returns relates to changes in expectations, whereas connectedness for volatilities captures the fear and uncertainty of investors.

While we highlight the differences between results when appropriate, we mainly focus on connectedness for volatilities, for two reasons. Firstly, when examining groups as well as individual ETMs, the static analysis of connectedness for volatilities and returns produces comparable results. Secondly, understanding volatility connectedness is critical for real-time crisis monitoring. In fact, volatilities tend to move together only during times of crises and are often more responsive than returns which, on the contrary, move together in both downturns and upswings. The full set of results is available in Appendix B.

[14]We have increased p up to 12, but this leads to a very low fraction of active coefficients, resulting in a highly sparse VAR. We conclude that 4 lags capture an adequate amount of autocorrelation in the case of returns, while for RV, exhibiting larger sparsity, 3 lags are sufficient. As a robustness check, we have also computed system-wide connectedness considering different horizons. Specifically, we set $H = 4, 6, 12$, and conclude that connectedness of both returns and RV is not particularly sensitive to the choice of H. These results are available from the authors upon request.

3.1 Full sample connecteness

Starting from the CT, we compute the From, To and Net connectedness for RV as defined in Equations (6), (7) and (8) respectively and display them in Figure 4 where base, precious and other ETMs are clustered and represented with different colors.

Figure 4: To, From and Net connectedntess – volatilities

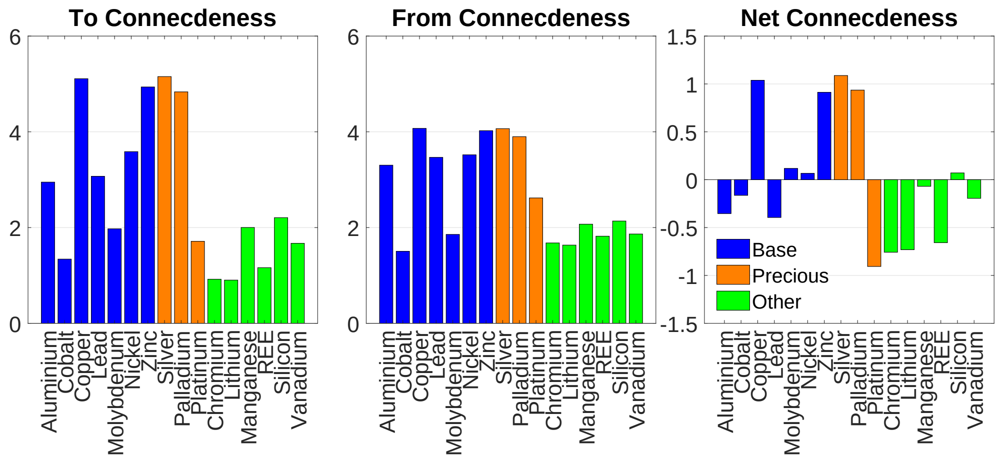

Base and precious metals exhibit greater From and To connectedness, whereas the other ETMs transmit and receive less volatility spillovers. Connectedness is thus stronger for the first two groups, while other ETMs are to some extent less sensitive to base and precious metal market dynamics. Moreover, other ETMs also exhibit a degree of From connectedness that is generally higher than the degree of To connectedness, suggesting that they are net receivers of shocks.

As a matter of fact, metals in the "other ETMs" group – with the exception of silicon – have a negative Net directional connectedness, and hence they are net receivers of volatility spillovers. On the contrary, two precious metals out of three - namely, silver and palladium - are net transmitters of shocks. Results for base minerals are mixed, with four out of seven metals being classified as net transmitters of shocks. It is worth noting that copper and zinc have the highest degree of From and To connectedness among base metals. When analysing spillovers for returns, copper is confirmed to be the most connected metal, thus it seems to be the principal driver of markets dynamics for ETMs.

We summarise the full-sample connectedness analysis for volatilities in Figure 5. The heatmap in Figure 5a represents the volatility CT for groups of ETMs. Within-group con-

Figure 5: Full sample group connectedness measures for volatility

(a) Within and cross group connectedness

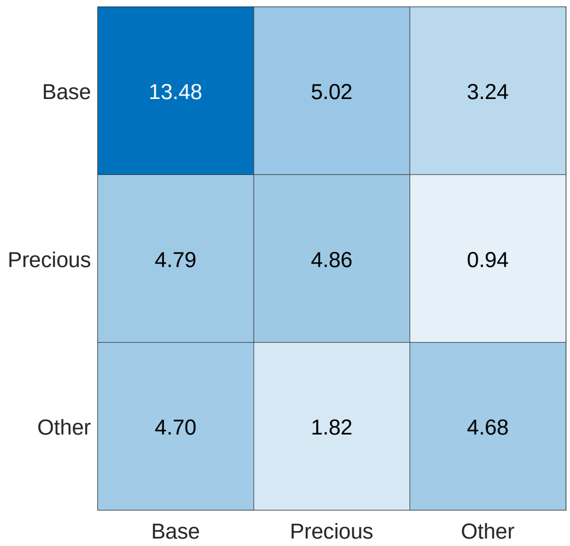

(b) To, From and Net connectedness

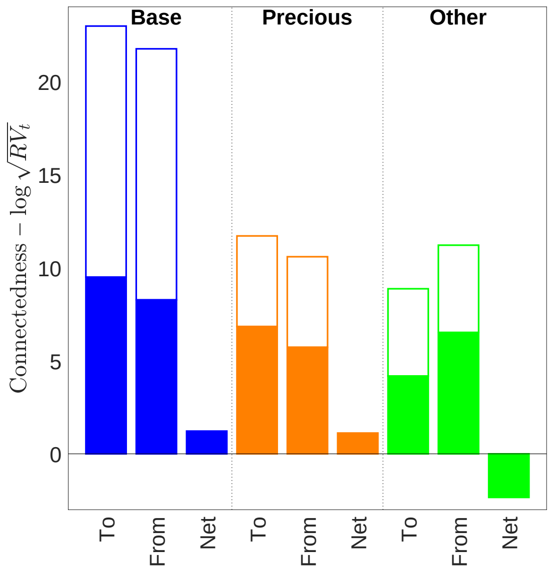

Notes: panel (a) shows within group connectedness along the main diagonal, while off-diagonal elements are cross group connectedness measures. Panel (b) shows the To, From and Net connectedness statistics for groups of metals. Colored areas refer to the off-diagonal statistics, whereas the white areas denote the statistics comprehending the diagonal elements.

nectedness (net of own connectedness for each metal) can be read along the main diagonal, while off-diagonal elements of the heatmap capture volatility spillovers across groups. Within-group spillovers are largest for base metals, while those for precious and other ETMs are much smaller and comparable in magnitude; this suggests that these two markets receive a large share of volatility spillovers from the base metal group. Figure 5b reports the To, From and Net group-connectedness, confirming the results obtained with individual commodities. Base and precious metals are overall net transmitters, while other ETMs are net receivers of shocks.

Some interesting facts also emerge from the CT for returns and RV, reported in Appendix B. Diagonal elements are in general lower for base and precious metals, and higher for minerals classified as "other ETMs". This means that other ETMs variability is more self-explained with respect to the other two metal categories. The only exception is molybdenum that, notwithstanding being classified as base metal, has a degree of self-explained volatility as high as other ETMs. Off-diagonal elements range from the very high levels of pairwise directional connectedness measured from zinc to lead and from palladium to platinum (more than 20%) to the marginal and often negligible connectedness arising from other ETM to base and precious metals (e.g. silicon and vanadium transmit around 1% of the RV to zinc and silver). Crucially, the opposite is not true, as the connectedness from any of the base and precious metals to other ETM is on average larger, denoting a remarkable asymmetry. Since the visualization of the pairwise connectedness measures is easier when represented via network graphs, the remainder of this discussion is delayed to Section 3.2.

Lastly, we focus on full-sample total or system-wide connectedness, as defined in Equation (9), which is equal to 44.93% for returns, and to 43.53% for RV. These results are in line with those of Diebold et al. (2018), estimating a total connectedness among commodity prices at 40%. This implies that almost half of metals variability uncertainty originates by "non-own" shocks. We can further disentangle total RV connectedness measuring within and between connectedness: 23.02% of the connectedness arises within the same group of ETMs, whereas the 20.51% of system-wide connectedness originates across groups.

3.2 Network visualisation

To better display the results, we consider the network representation of the CT in Figure 6.[15]

To improve the network visualisation, we rely on Net-Pairwise statistics C_{ij} to determine the arrow direction that points towards net receivers of shocks. We use the ForceAtlas2 algorithm (Jacomy et al., 2014) that finds an equilibrium in which repelling and attractive forces among nodes are balanced. The nodes naturally repulse each other, whereas links attract nodes with different forces, proportional to Net-Pairwise connectedness.

It is interesting to note that, even though we provide three *ex-ante* defined clusters, the completely data-driven algorithm groups together the base, precious and other ETM metals, both in the case of returns and RV analyses. The only exceptions are given by molybdenum and cobalt, considered as base metals by the IMF but part of the other ETMs according to the connectedness features both in the case of RV and returns.

As for RV connectedness, shown in Figure 6b, chromium, REE and lithium are closer

[15]To produce network graphs, we use the Gephi open-access software available at `https://gephi.org/`.

Figure 6: Network visualisation for ETMs returns and RV connectedness – June 2012 - December 2022

(a) Returns (b) Volatilities

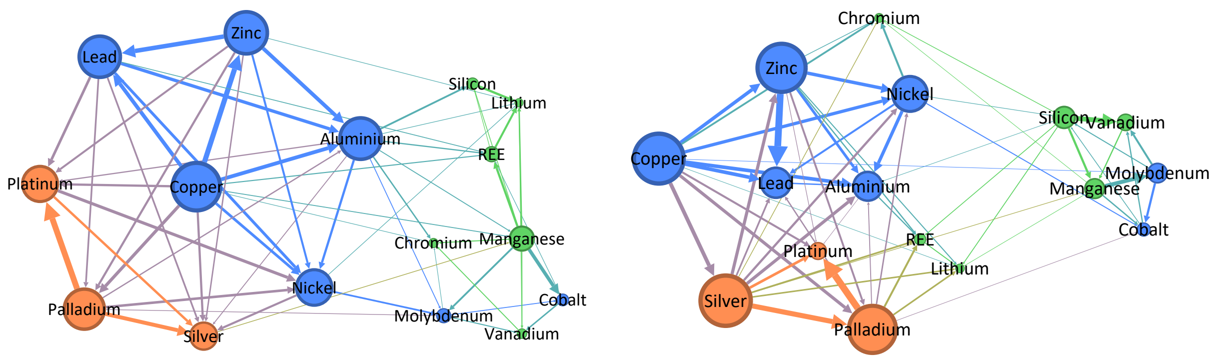

Notes: size of the nodes is determined by To connectedness. Arrows and edges refer to the Net-Pairwise connectedness above the median. Node colour reflects the grouping of metals into base (blue), precious (orange), and others (green).

to base and precious metals, whereas when analysing connectedness in returns, they are grouped among the other ETMs. Base and precious metals have more weight in the network and are more connected than other ETMs. This can be appreciated by focusing on the size of the nodes and the number of arrows originating from each node, respectively.

3.3 Dynamic rolling sample connectedness

Static connectedness provides useful tools to measure the average degree of connectedness over the sample; however previous analyses show that such measures are usually time-varying. Figure 7 reports system-wide returns and volatility connectedness obtained by estimating VAR models over a rolling window.[16] The figure also reports vertical lines in correspondence of key events that are expected to affect connectedness.

Return connectedness from mid-2017 is always above the static full-sample average of 44.93%, suggesting that connectedness among the ETMs was lower in the beginning of the sample (i.e. 2012 – mid-2017) and has recently increased. Before the Covid-19 pandemic, return connectedness seems on a slightly decreasing path, while after reaching a minimum

[16]We set, as for the static full-sample analysis, a VAR(4) in the case of returns and a VAR(3) for RV, using a rolling window of 60 observations. Finally, we consider $H = 3, 4, 6, 12$, but report only results for $H = 3$ given the marginal and negligible differences in the estimated connectedness.

at the end of 2019, there is again a surge in total connectedness among ETMs. Volatility connectedness follows a similar patterns but displays more variability. It is downward sloped until the end of 2020. Thereafter, system-wide connectedness of ETMs RV is on an increasing trend. Surprisingly, we do not find evidence for an increase in RV connectedness during the only recession within our sample. This may be due to the particular features of the 2020/21 slowdown, characterised by high levels of uncertainty but also by an umprecedent economic freezing (i.e. production, trade and consumption dramatically dropped, affecting almost all markets around the world).

Figure 7: Retuns and volatility connectedness - rolling sample

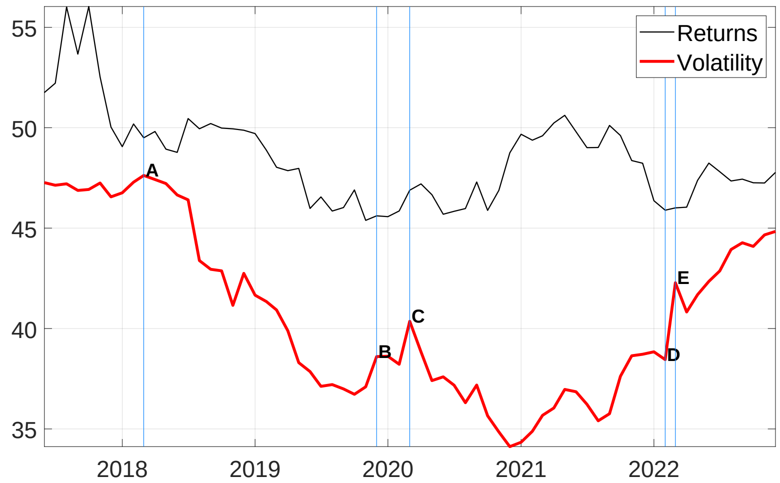

- A: 2018:03 - Tarrifs on Aluminium
- B: 2019:12 - Brexit
- C: 2020:03 - Covid
- D: 2022:02 - War in Ukraine
- E: 2022:03 - Nickel short squeeze

Nevertheless, RV connectedness does exhibit spikes in correspondence of key economic and geo-political events. On the contrary, connectedness for returns seems to be less responsive. The announcement of tarrifs on US aluminium imports by president Trump in March 2018 and the nickel short squeeze in the London Metal Exchange March 2022 are both associated with a decrease in RV connectedness. RV connectedness also decreases in correspondence of Britain's General Election in December (i.e. that with the victory of the conservatory party meant the confirmation Brexit) and the outbreak of the Covid-19 pandemic in March 2020. On the contrary, we see that in correspondence of the Russian invasion of ukraine in February 2022, RV connectedness rapidly rises. The effect is then confounded by the response to the nickel short squeeze in March 2022.[17]

[17]See e.g.: `https://internationalbanker.com/brokerage/the-nickel-short-squeeze-what-happened/`

We consider rolling-sample within- and between-group connectedness for both returns and RV in Figure 8. It is interesting to note that in both cases, the total connectedness mimic the evolution of the between-group connectedness, meaning that spillovers across- rather than within-groups are key in shaping the final time-varying system-wide connectedness.

Figure 8: Time-varying Connectedness: total, within and between groups

(a) Returns (b) $log\sqrt{RV_t}$

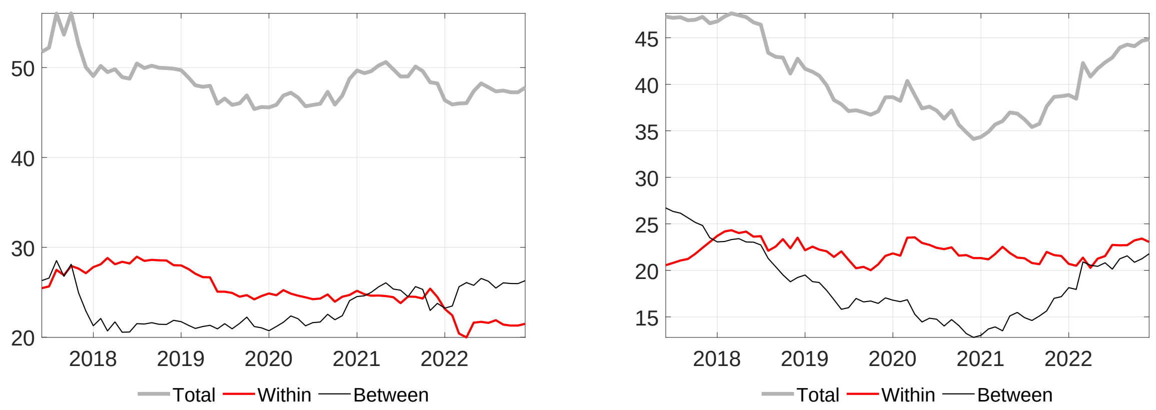

Lastly, Figure 9 shows the evolution of the Net connectedness for each group of metals. Overall, the dynamics of the total connectedness in returns or RV (Figure 7) are closer to the Net connectedness of base metals, which shows almost the same pattern. On the contrary, the evolution of precious metals and other ETMs net connectedness is not in line with the fluctuations of total connectedness, neither considering returns nor volatilities. We believe this is a further confirmation of the relative importance of base metals within ETMs.

Figure 9: Time-varying net connectedness by groups

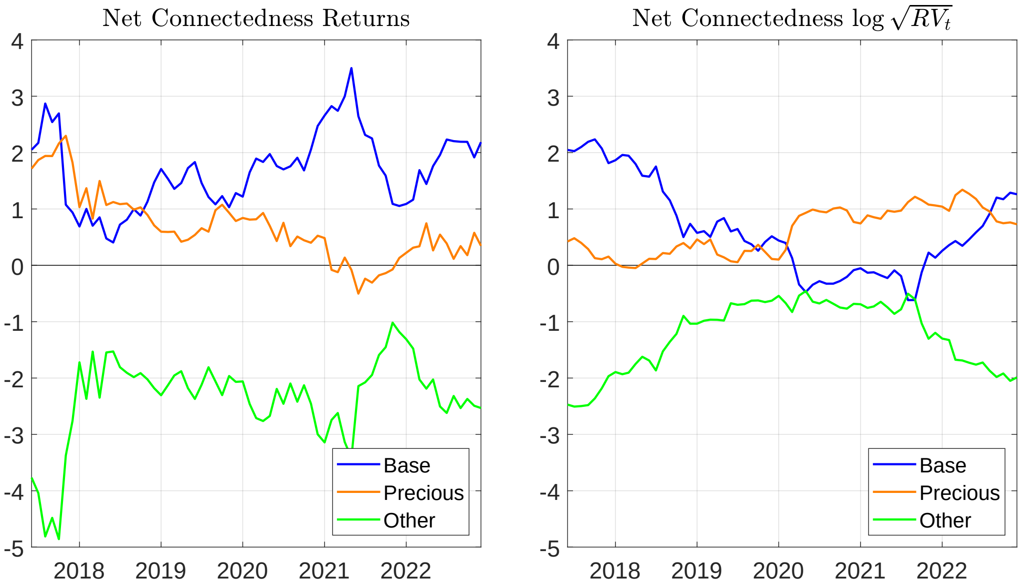

3.4 Connectedness and macroeconomic variables

To better understand the drivers of total connectedness, we consider its correlation with different macoreconomic variables. Specifically, since connectedness in returns should be associated to fluctuations in the business cycle, we focus on the correlation between the estimated time-varying return connectedness (C_t^{ret}) and the Global Economic Conditions Indicator (GECON) of Baumeister et al. (2022). We further examine the correlation between C_t^{ret} and the Global Supply Chain Pressure Index (GSCPI) of Benigno et al. (2022), since this proxy should capture fluctuations strongly associated with commodities, including ETMs.

As for RV connectedness (C_t^{RV}), we focus on measures of economic uncertainty. In particular, we analyse the correlation of C_t^{RV} with the Global Economic Policy Uncertainty (GEPU) index (Davis, 2016) and the Trade Policy Uncertainty (TPU) indicator proposed by Caldara et al. (2020).[18] Figure 10 shows the selected indices together with returns and RV time varying connectedness measures.

Interestingly, connectedness for returns increases during the Covid-induced recession of 2020, when the GECON index exhibits a severe drop. After the Covid-19 pandemic, how-

[18]We also consider the VIX index, but since its dynamics are similar to the evolution of the GEPU, we show results considering the GEPU only.

Figure 10: Time-varying connectedness, economic activity, uncertainty and supply chain pressure

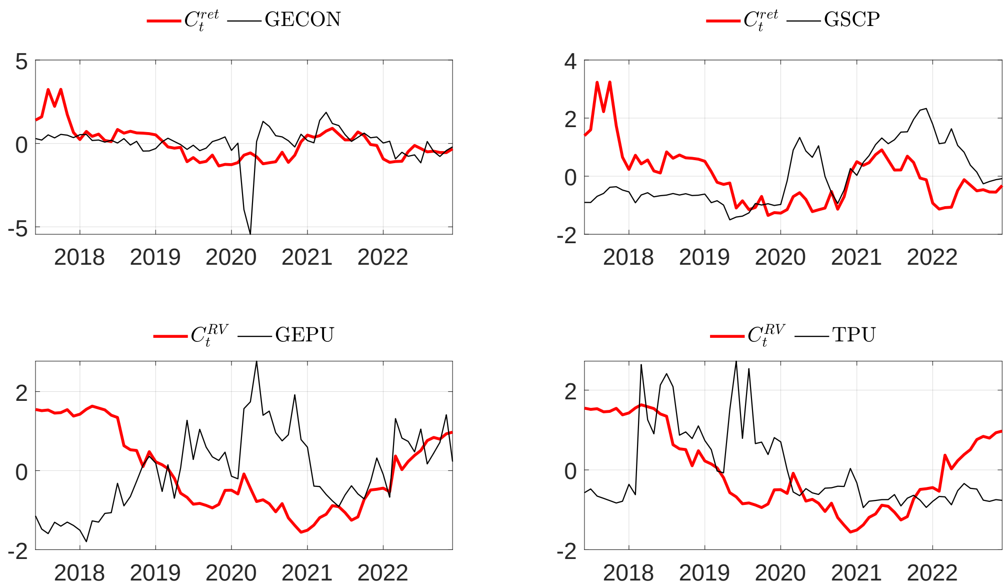

ever, the degree of connectedness for returns seems positively correlated with the economic activity (top-left panel). A simple leads-and-lags analysis between the GECON index and our measure for returns connectedness, C_t^r, reveals that the correlation coefficient is indeed positive and statistically significant at all lags and leads we consider (see Figure B3). On the contrary, we fail to detect statistically significant correlation between connectedness for ETMs returns and the global supply-chain pressure (Figure 10, top-right panel).

Focusing on the RV connectedness, it is clearly shown that, whereas at the beginning of the sample C_t^{RV} negatively correlates with economic uncertainty, starting from the mid-2021 the two indicators are both on a rising trend (bottom-left panel).[19] The correlation between C_t^{RV} and the GEPU indicator is negative sign and is only statistically significant when considering lags, that is, volatility connectedness is influenced by global economic uncertainty, but the effect takes some months to manifest. The higher economic uncertainty is, the lower system-wide connectedness becomes after some periods, suggesting that markets interconnection decreases after periods of great uncertainty. On the contrary, it is hard to detect some kind of co-movement between the trade policy uncertainty indicator and ETMs

[19] A similar behaviour is observed also for the VIX index.

volatility connectedness (Figure 10, bottom-right panel).

It is possible that the leads-and-lags analysis results are sensitive to different sub-sample definitions and that correlation between the time-varying connectedness and the selected measures in Figure 10 changes with time. However, since the set of observations is already limited, we find it hasty to analyse subsets of the five years span. Our conclusion is that the only significant drivers of the system-wide connectedness for the period of interest are business cycle fluctuations summarized by GECON in the case of returns and economic policy uncertainty as measures by GEPU for volatilities (see Figure B3).

3.5 Alternative measures of connectedness

As a robustness check, we compare our methodology with an alternative measure of connectedness suggested by Billio et al. (2012). Specifically we derive the time-varying system-wide connectedness for returns and volatilities relying on a principal component analysis (PCA). Billio et al. (2012) show that in a highly connected system, a small number of principal components is sufficient to explain most of the volatility of the entire system, thus constituting a valid alternative to the connectedness measure proposed by Diebold and Yilmaz (2009). To make a comparison, we extract the first two principal components as the major drivers of returns and volatilities over the rolling sample and plot the share of variance explained by the components.

Results in top panel of Figure 11 show the percent of variability explained by the first principal component and our baseline measure of connectedness, normalized to have the same mean and standard deviation of the PCA-based measure. We can see that for what concerns volatilities the two proxies are strikingly similar. As for returns, the similarity increases adding also the second principal component (bottom panel).

Figure 11: Alternative measures of time-varying connectedness

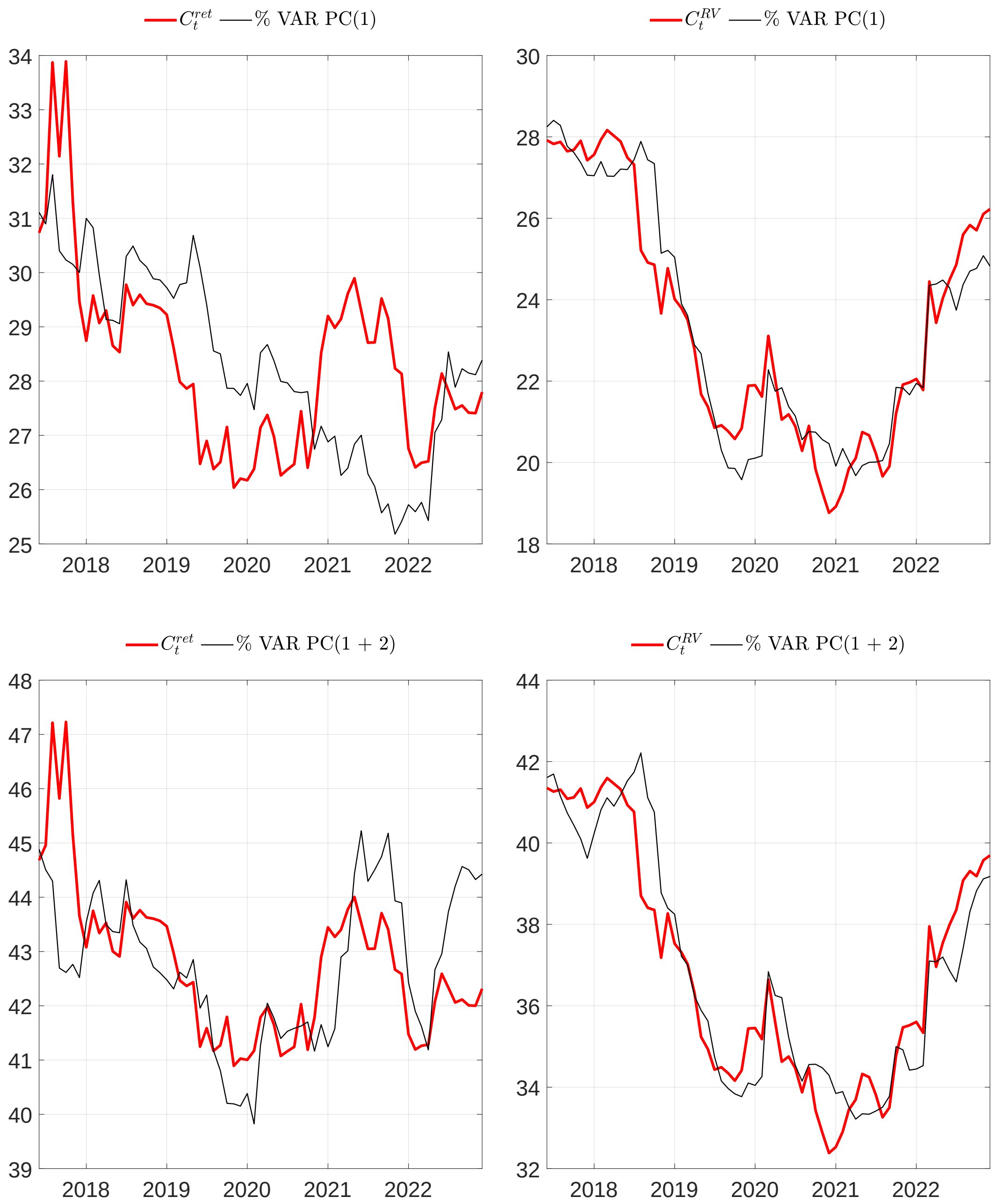

Notes: in top panel, C_t^{ret} and C_t^{RV} have been rescaled to ease the comparison. % VAR PC(1) represents the share of variance explained by the first principal component. % VAR PC(1+2) represents the share of variance explained by the first two principal components.

4 Conclusions

To combat climate change, countries have engaged in a historical effort to reduce greenhouse gas emissions. Among the necessary conditions for the success of these efforts are the substitution of fossil fuels with renewable energy sources in energy technologies for power generation, industry, mobility, buildings. This substitution entails at the same time a substantial increase in the demand for metals such as copper, nickel, cobalt, and lithium, which are key building blocks of the energy transition. For example, an electric car requires five times more of these metals than a conventional car.

The problem governments, companies, experts, public opinions are becoming increasingly aware of is that a more mineral-intensive global economy raises concerns that supply might not catch up with soaring demand. Shocks to the price of minerals as inputs could result from cost increases due to supply shocks but also from demand pressure. Countries that are material-dependent could be especially adversely affected. This is familiar terrain. The macroeconomic consequences of oil shocks are well understood by both economists and policy makers.

The case of critical raw materials, and of energy transition metals in particular, presents a few significant differences, though. Shocks that can occur along the supply chain of materials will have macroeconomic impacts on material-dependent economies (possibly on material-rich countries as well). Unlike oil and gas, however, several minerals are exchanged in thin illiquid markets, increasing the volatility of prices and making it difficult for traders to hedge risks. In addition, besides economic and financial aspects, for minerals there is an environmental problem as the above-mentioned difficulties may, perhaps significantly, delay the energy transition.

The other important difference is that, while there is only one oil (and gas) there are many minerals that are critical for carrying out the energy transition within a relatively short horizon. This paper presents evidence that these minerals tend to bind together. In this paper we provide quantitative evidence on the spillovers that characterise a set of metals that are critical for the challenge represented by the radical change of energy sectors required by the goal of net zero emissions and the decarbonisation of economies. These are 16 metals that constitute the IMF's Energy Transition Metals index and are comprised of three groups: Base, Precious, and Other metals. We compute returns and realised volatilities and estimate spillovers among them by relying on the connectedness approach pioneered by Diebold and Yilmaz (2009, 2012, 2014). Specifically, we estimate a sparse VAR with an elastic-net structure and construct our connectedness measures from the Generalised

Forecast Error Variance Decomposition, which is independent from variables ordering.

The static full-sample connectedness analysis shows that the Base and Precious metal groups transmit shocks to the Other ETMs that are net receivers. By splitting the 16 commodities in three groups we show that almost half of the connectedness originates within each group, whereas the other half is due to cross-group spillovers.

Considering the dynamics of connectedness, obtained with a rolling window estimation of the VAR, we find that the system-wide volatility connectedness has increased after the COVID-19 outbreak. Moreover, the system-wide connectedness of ETM returns is positively correlated with the economic activity, whereas volatility connectedness seems to be more related to global economic policy uncertainty. Finally, alternative measures of connectedness may lead to slightly different results, but our results seem overall robust to the different definition of connectedness based on principal components.

The deployment of low-carbon energy technologies is expected to make the energy-mineral nexus ever more important. This is because these emerging technologies, characterized by a potential to mitigate global warming, require specific mineral resources in significant quantities which makes resource depletion a real concern. Because nearly all clean energy technologies employ several critical minerals, the degree of interconnection among them is relevant information and so is the pattern of transmission of potential shocks for both managers and policymakers.

References

Acemoglu, D., Carvalho, V. M., Ozdaglar, A., and Tahbaz-Salehi, A. (2012). The network origins of aggregate fluctuations. *Econometrica*, 80(5):1977–2016.

Ahmadi, M. and Manera, M. (2021). Oil price shocks and economic growth in oil-exporting countries. *FEEM Working Paper*.

Andersen, T. G., Bollerslev, T., Diebold, F. X., and Ebens, H. (2001). The distribution of realized stock return volatility. *Journal of financial economics*, 61(1):43–76.

Balcilar, M., Usman, O., and Agan, B. (2022). On the connectedness of commodity markets: A critical and selective survey of empirical studies and bibliometric analysis. *Journal of Economic Surveys*, *forthcoming*.

Bandt, O. D., Hartmann, P., and Peydró, J. L. (2012). Systemic Risk in Banking: An Update. In Berger, A. N., Molyneux, P., and Wilson, J. O. S., editors, *The Oxford Handbook of Banking*, chapter 25, page 633–672. Oxford University Press.

Barigozzi, M. and Brownlees, C. (2019). Nets: Network estimation for time series. *Journal of Applied Econometrics*, 34(3):347–364.

Barigozzi, M., Cavaliere, G., and Moramarco, G. (2022). Factor network autoregressions. *arXiv preprint arXiv:2208.02925*.

Baruník, J. and Kley, T. (2019). Quantile coherency: A general measure for dependence between cyclical economic variables. *The Econometrics Journal*, 22(2):131–152.

Baruník, J. and Křehlík, T. (2018). Measuring the frequency dynamics of financial connectedness and systemic risk. *Journal of Financial Econometrics*, 16(2):271–296.

Bastianin, A., Galeotti, M., and Manera, M. (2017). Oil supply shocks and economic growth in the Mediterranean. *Energy Policy*, 110:167–175.

Baumeister, C., Korobilis, D., and Lee, T. K. (2022). Energy markets and global economic conditions. *Review of Economics and Statistics*, 104(4):828–844.

Benigno, G., Di Giovanni, J., Groen, J. J., and Noble, A. I. (2022). The GSCPI: a new barometer of global supply chain pressures. Staff Report 1017, Federal Reserve Bank of New York.

Berument, M. H., Ceylan, N. B., and Dogan, N. (2010). The impact of oil price shocks on the economic growth of selected mena1 countries. *The Energy Journal*, 31(1).

Billio, M., Getmansky, M., Lo, A. W., and Pelizzon, L. (2012). Econometric measures of connectedness and systemic risk in the finance and insurance sectors. *Journal of financial economics*, 104(3):535–559.

Boer, L., Pescatori, A., and Stuermer, M. (2021). Energy transition metals. Working Paper 243, International Monetary Fund.

Caldara, D., Iacoviello, M., Molligo, P., Prestipino, A., and Raffo, A. (2020). The economic effects of trade policy uncertainty. *Journal of Monetary Economics*, 109:38–59.

Davis, S. J. (2016). An index of global economic policy uncertainty. Technical report, National Bureau of Economic Research.

Diebold, F. X., Liu, L., and Yilmaz, K. (2018). Commodity Connectedness. In Mendoza, E. G., Pastén, E., and Saravia, D., editors, *Monetary Policy and Global Spillovers: Mechanisms, Effects and Policy Measures*, volume 25 of *Central Banking, Analysis, and Economic Policies Book Series*, chapter 4, pages 97–136. Central Bank of Chile.

Diebold, F. X. and Yilmaz, K. (2009). Measuring financial asset return and volatility spillovers, with application to global equity markets. *The Economic Journal*, 119(534):158–171.

Diebold, F. X. and Yilmaz, K. (2012). Better to give than to receive: Predictive directional measurement of volatility spillovers. *International Journal of forecasting*, 28(1):57–66.

Diebold, F. X. and Yilmaz, K. (2014). On the network topology of variance decompositions: Measuring the connectedness of financial firms. *Journal of Eeconometrics*, 182(1):119–134.

Diebold, F. X. and Yilmaz, K. (2023). On the past, present, and future of the Diebold-Yilmaz approach to dynamic network connectedness. *Journal of Econometrics*, *forthcoming*.

Esfahani, H. S., Mohaddes, K., and Pesaran, M. H. (2014). An empirical growth model for major oil exporters. *Journal of Applied Econometrics*, 29(1):1–21.

European Commission (2020a). Critical raw materials for strategic technologies and sectors in the EU - A foresight study. Available online at: `https://ec.europa.eu/docsroom/documents/42881`.

European Commission (2020b). Critical raw materials resilience: Charting a path towards greater security and sustainability. COM(2020) 474. Available online at: `https://ec.europa.eu/docsroom/documents/42849`.

Fally, T. and Sayre, J. (2018). Commodity trade matters. NBER Working Paper 24965, National Bureau of Economic Research.

French, K. R., Schwert, G. W., and Stambaugh, R. F. (1987). Expected stock returns and volatility. *Journal of financial Economics*, 19(1):3–29.

Garcia, C. J. and González, W. D. (2013). Exchange rate intervention in small open economies: The role of risk premium and commodity price shocks. *International Review of Economics & Finance*, 25:424–447.

Graedel, T. E., Harper, E. M., Nassar, N. T., Nuss, P., and Reck, B. K. (2015a). Criticality of metals and metalloids. *Proceedings of the National Academy of Sciences*, 112(14):4257–4262.

Graedel, T. E., Harper, E. M., Nassar, N. T., and Reck, B. K. (2015b). On the materials basis of modern society. *Proceedings of the National Academy of Sciences*, 112(20):6295–6300.

Hamilton, J. D. (2009). Causes and consequences of the oil shock of 2007-08. *NBER Working Paper.*

Hoerl, A. and Kennard, R. (1988). Ridge regression. In *Encyclopedia of Statistical Sciences*, volume 8. Wiley.

Jacomy, M., Venturini, T., Heymann, S., and Bastian, M. (2014). Forceatlas2, a continuous graph layout algorithm for handy network visualization designed for the gephi software. *PloS one*, 9(6):e98679.

Kilian, L. (2008). The economic effects of energy price shocks. *Journal of economic literature*, 46(4):871–909.

Kilian, L. (2009). Not all oil price shocks are alike: Disentangling demand and supply shocks in the crude oil market. *American Economic Review*, 99(3):1053–1069.

Kinda, T., Mlachila, M., and Ouedraogo, R. (2018). Do commodity price shocks weaken the financial sector? *The World Economy*, 41(11):3001–3044.

Koop, G., Pesaran, H. M., and Potter, S. M. (1996). Impulse response analysis in nonlinear multivariate models. *Journal of Econometrics*, 74(1):119–147.

Lèbre, É., Stringer, M., Svobodova, K., Owen, J. R., Kemp, D., Côte, C., Arratia-Solar, A., and Valenta, R. K. (2020). The social and environmental complexities of extracting energy transition metals. *Nature Communications*, 11(1):4823.

Metcalf, G. E. (2014). The economics of energy security. *Annu. Rev. Resour. Econ.*, 6(1):155–174.

Nakano, J. (2021). The geopolitics of critical minerals supply chains. Center for Strategic and International Studies (CSIS). Available online at: `http://www.jstor.org/stable/resrep30033`.

Nicholson, W. B., Matteson, D. S., and Bien, J. (2017). VARX-L: Structured regularization for large vector autoregressions with exogenous variables. *International Journal of Forecasting*, 33(3):627–651.

Owen, J. R., Kemp, D., Lechner, A. M., Harris, J., Zhang, R., and Lèbre, É. (2022). Energy transition minerals and their intersection with land-connected peoples. *Nature Sustainability*, pages 1–9.

Peersman, G. and Van Robays, I. (2012). Cross-country differences in the effects of oil shocks. *Energy Economics*, 34(5):1532–1547.

Pesaran, H. M. and Shin, Y. (1998). Generalized impulse response analysis in linear multivariate models. *Economics Letters*, 58(1):17–29.

Sekine, A. and Tsuruga, T. (2018). Effects of commodity price shocks on inflation: A cross-country analysis. *Oxford Economic Papers*, 70(4):1108–1135.

Sovacool, B. K. and Brown, M. A. (2010). Competing dimensions of energy security: an international perspective. *Annual Review of Environment and Resources*, 35:77–108.

Tibshirani, R. (1996). Regression shrinkage and selection via the lasso. *Journal of the Royal Statistical Society: Series B (Methodological)*, 58(1):267–288.

U.S. Department of the Interior (2022). 2022 Final list of critical minerals. Federal Register, 87 FR 10381, 10381-10382. Available online at: `https://www.federalregister.gov/documents/2022/02/24/2022-04027/2022-final-list-of-critical-minerals`.

Yergin, D. (2006). Ensuring energy security. *Foreign affairs*, 85(2):69–82.

Zhang, L., Chen, Z., Yang, C., and Xu, Z. (2022). Global supply risk assessment of the metals used in clean energy technologies. *Journal of Cleaner Production*, 331:129602.

Zhu, X., Wang, W., Wang, H., and Härdle, W. K. (2019). Network quantile autoregression. *Journal of econometrics*, 212(1):345–358.

Zou, H. and Zhang, H. H. (2009). On the adaptive elastic-net with a diverging number of parameters. *Annals of Statistics*, 37(4):1733–1751.

A Descriptive statistics

Here we report the log of the realised volatility in standard deviations for the 16 ETMs over the entire sample (Figure A1) and additional information considering aggregation of the 16 commodities in three groups. In particular, Figure A2 shows the price indices and the RV for each group (base metals, precious metals, other ETMs). Finally, Table A1 describes the IMF nominal commodity price indices used in the analysis.

Figure A1: Log realised volatility of energy transition metals: June 2012 - December 2022

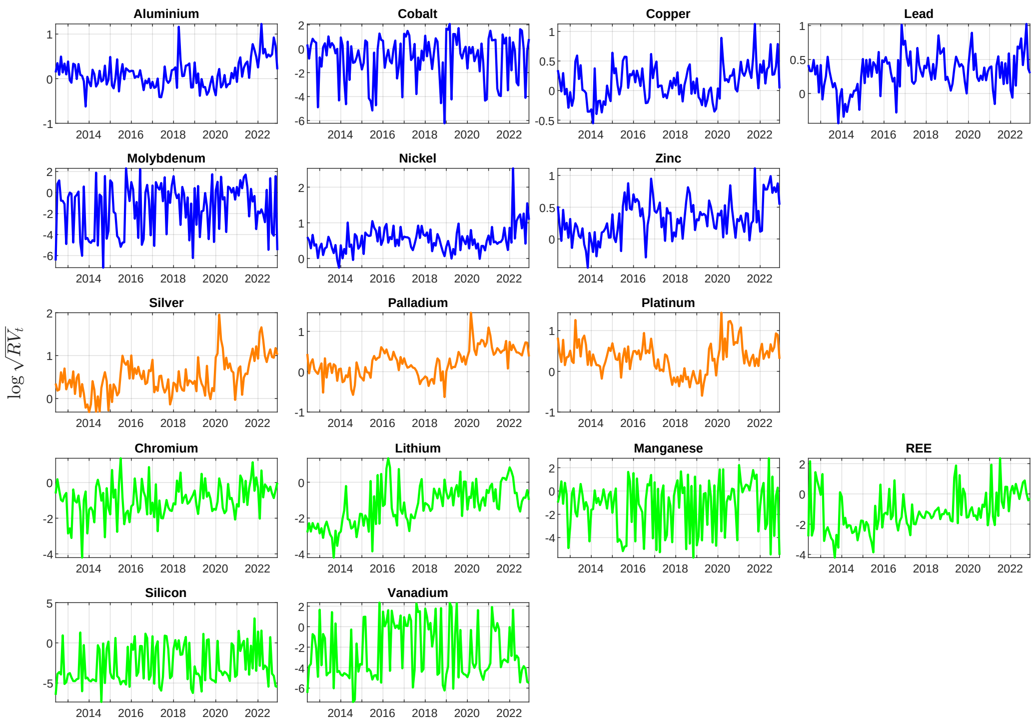

Figure A2: Energy Transition, Base, Precious and Other Metals: price indices and volatilities June 2012 - December 2022

(a) Price indices

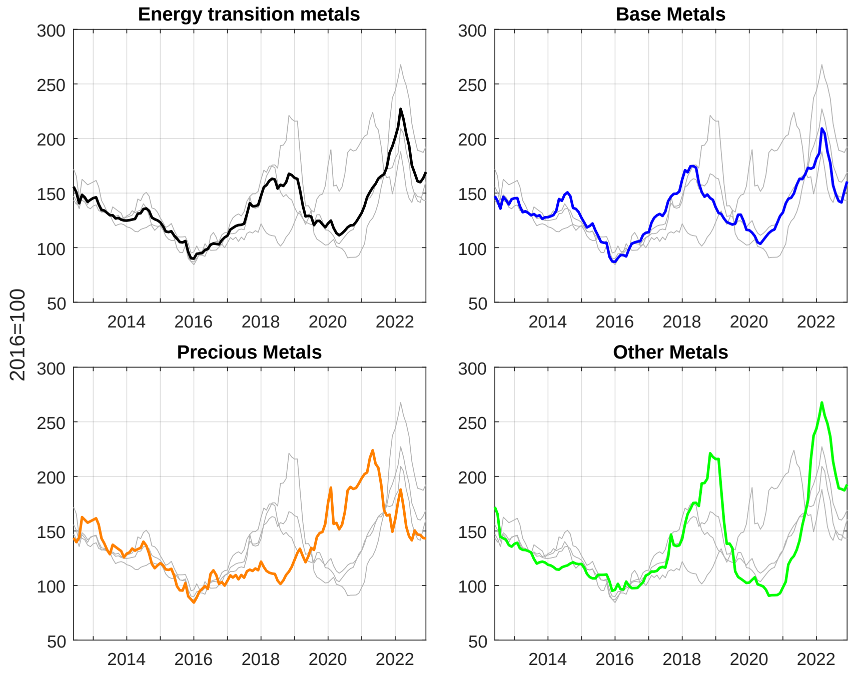

(b) Log Realized Volatilities

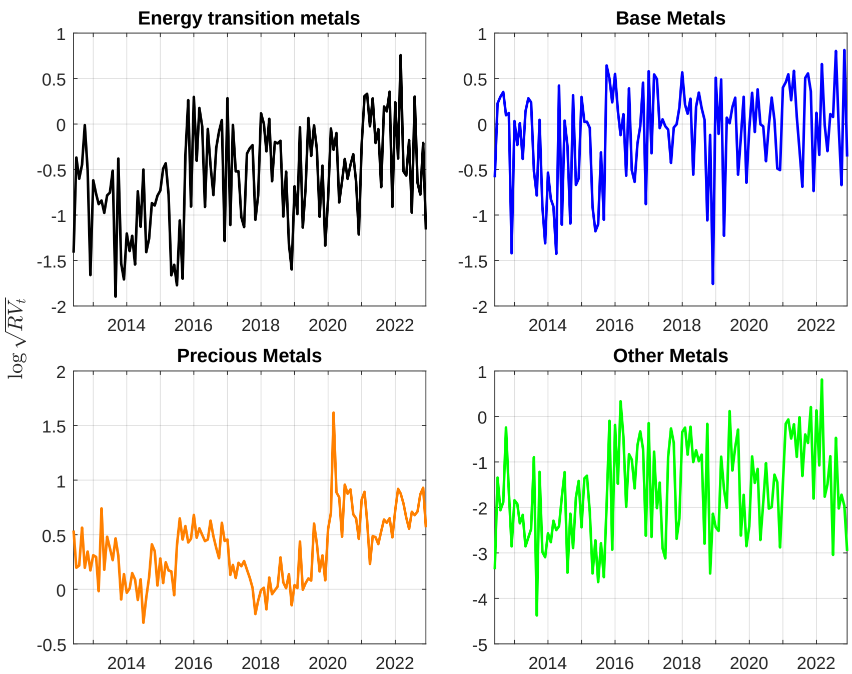

Notes: price indices and log realised standard deviations for each category of metals. Price indices and volatilities shown in the graphs are computed as cross-sectional averages of the underlying series. Prices have been normalized as follows: $100 \times P_{mt}/\bar{P}_m^{2016}$ where $\bar{P}_m^{2016}$ is the average price of m for 2016. Metal groups are defined in Table 1.

Table A1: IMF Price indices and commodity price indices: metals

Commodity/Index	Group	Metal Group	Type	Unit	Details	Source
Base Metals Price Index	MET	BM	Index	2016 = 100		IMF
Energy Transition Metal Index	MET	ETM	Index	2016 = 100		IMF
Precious Metals Price Index	MET	PM	Index	2016 = 100		IMF
Aluminum	MET	ETM, BM	Price	USD/Metric Ton	99.5% min purity LME spot price CIF UK ports	LME
Chromium	ETM	ETM	Price	USD/Metric Ton	Chromium 99.2% Coarse Particle	Shanghai ME
Cobalt	MET	ETM, BM	Price	USD/Metric Ton	minimum 99.80% purity LME spot price	LME
Copper	MET	ETM, BM	Price	USD/Metric Ton	grade A cathode LME spot price, CIF European ports	LME
Lead	MET	ETM, BM	Price	USD/Metric Ton	99.97% pure LME spot price, CIF European Ports	LME
Lithium	ETM	ETM	Price	USD/Metric Ton	Lithium Metal 99% Battery Grade	Shanghai ME
Manganese	ETM	ETM	Price	USD/Metric Ton	Manganese Electro CIF NWE	Refinitiv
Molybdenum	MET	ETM, BM	Price	USD/Metric Ton	57 %-63% purity roasted molybdenum concentrate	Refinitiv
Nickel	MET	ETM, BM	Price	USD/Metric Ton	melting grade LME spot price, CIF European ports	LME
Palladium	MET	ETM, PM	Price	USD/troy ounce	Palladium LME spot price	LME
Platinum	MET	ETM, PM	Price	USD/troy ounce	Platinum LME spot price	LME
Rare Earth Elements	ETM	ETM	Price	USD/Metric Ton	Rare Earth Carbonate REO 42-45 Dom	Shanghai ME
Silicon	ETM	ETM	Price	USD/Metric Ton	Silicon Lumps, CIF NWE	Refinitiv
Silver	MET	ETM, PM	Price	USD/troy ounce	London Bullion Market Association	ICE
Vanadium	ETM	ETM	Price	USD/Metric Ton	Vanadium Pentoxide, CIF NWE	Refinitiv
Zinc	MET	ETM, BM	Price	USD/Metric Ton	high grade 98% pure	LME

B Additional tables and figures

This Section reports the connectedness tables for returns and RV of the 16 ETMs (Tables B1 and B2). Additionally, Figures B1 and B2 focus on From, To and Net connectedness statistics for returns, not reported in the paper. Figure B3 reports the leads and lags correlation analysis between the estimated connectedness and some selected indicators of economic activity, uncertainty and supply-chain pressure.

Table B1: Connectedness table for returns

	Base							Precious			Other						
	Aluminium	Cobalt	Copper	Lead	Molybdenum	Nickel	Zinc	Silver	Palladium	Platinum	Chromium	Lithium	Manganese	REE	Silicon	Vanadium	From
Aluminium	36.57	0.13	12.38	10.66	0.79	6.80	12.47	2.25	4.19	3.65	1.84	0.99	0.91	2.43	3.55	0.40	3.96
Cobalt	1.57	72.17	1.42	1.82	2.88	1.03	1.10	0.66	1.16	0.92	0.27	0.31	11.32	1.36	0.36	1.65	1.74
Copper	10.83	0.03	31.43	11.27	0.02	7.15	15.78	4.82	9.18	6.11	0.67	0.05	0.64	1.55	0.17	0.31	4.29
Lead	10.08	0.42	12.33	34.55	0.17	8.08	14.53	4.23	5.53	7.82	0.33	0.12	0.01	1.31	0.07	0.43	4.09
Molybdenum	2.82	1.44	1.59	1.61	71.70	5.70	1.35	0.79	2.37	1.40	1.28	0.23	6.09	0.82	0.06	0.75	1.77
Nickel	7.45	0.06	8.87	9.40	2.39	38.20	6.69	5.72	8.26	9.96	0.02	1.19	0.07	0.89	0.46	0.37	3.86
Zinc	11.49	0.02	16.73	14.06	0.13	5.80	33.37	3.28	6.65	5.74	0.67	0.97	0.10	0.52	0.23	0.24	4.16
Silver	2.99	0.44	7.13	5.70	0.15	6.87	4.58	46.34	12.84	7.87	1.05	0.08	1.64	0.51	0.99	0.82	3.35
Palladium	4.13	0.01	10.37	5.71	0.56	7.53	7.07	9.83	35.35	18.16	0.00	0.17	0.01	0.61	0.15	0.34	4.04
Platinum	3.92	0.08	7.38	8.57	0.36	9.67	6.51	6.46	19.22	37.19	0.06	0.02	0.10	0.30	0.10	0.07	3.93
Chromium	4.52	1.01	1.95	0.78	1.85	0.26	1.75	1.77	0.17	0.13	77.60	0.85	3.32	0.53	0.47	3.04	1.40
Lithium	2.05	0.60	0.36	0.34	0.61	2.09	2.02	0.68	0.38	0.03	1.24	69.02	4.55	6.71	7.51	1.83	1.94
Manganese	2.98	5.31	2.88	1.54	5.93	1.08	1.34	2.51	0.87	0.90	2.23	0.27	68.66	2.02	0.36	1.10	1.96
REE	3.99	2.08	3.46	2.75	1.64	1.03	0.75	1.74	1.25	0.48	0.56	3.05	7.19	67.22	1.70	1.08	2.05
Silicon	5.96	0.50	0.56	0.21	0.34	0.35	0.62	1.09	0.29	0.13	1.07	0.09	2.45	1.97	84.07	0.31	1.00
Vanadium	1.05	4.80	0.74	0.95	3.44	0.83	0.54	1.52	0.78	0.22	0.63	1.73	3.10	1.73	0.27	77.67	1.40
To	4.74	1.06	5.51	4.71	1.33	4.02	4.82	2.96	4.57	3.97	0.74	0.63	2.59	1.45	1.03	0.80	**44.93**
Net	0.77	-0.68	1.22	0.62	-0.44	0.15	0.65	-0.39	0.53	0.04	-0.66	-1.30	0.63	-0.59	0.03	-0.60	-

Notes: full sample connectedness. Entry in bold is total connectedness.

Table B2: Connectedness table for volatilities

	Base							Precious			Other						
	Aluminium	Cobalt	Copper	Lead	Molybdenum	Nickel	Zinc	Silver	Palladium	Platinum	Chromium	Lithium	Manganese	REE	Silicon	Vanadium	From
Aluminium	47.15	0.02	11.18	4.23	0.23	10.11	8.35	9.64	2.88	1.05	0.71	0.27	0.59	2.43	1.10	0.08	3.30
Cobalt	0.05	75.93	0.86	0.12	6.92	3.11	0.37	0.32	1.63	0.12	0.75	0.03	4.16	0.59	2.24	2.80	1.50
Copper	8.26	0.39	34.86	8.75	0.71	8.03	10.51	11.73	9.01	3.81	2.71	0.71	0.17	0.24	0.05	0.08	4.07
Lead	3.99	0.07	11.18	44.54	0.20	6.14	21.17	5.36	4.05	0.81	0.78	0.58	0.38	0.70	0.00	0.04	3.47
Molybdenum	0.37	6.72	1.45	0.31	70.30	0.31	0.69	0.17	1.26	0.02	0.19	0.31	12.16	0.12	1.40	4.22	1.86
Nickel	9.37	1.77	10.06	6.02	0.17	43.69	10.48	7.05	4.38	0.37	3.76	0.32	0.02	0.64	1.23	0.67	3.52
Zinc	6.30	0.17	10.74	16.92	0.34	8.54	35.61	9.79	5.67	1.23	1.11	1.49	0.08	1.90	0.01	0.08	4.02
Silver	7.15	0.14	11.76	4.21	0.07	5.64	9.61	34.95	14.58	4.93	1.10	2.25	1.05	2.55	0.02	0.01	4.07
Palladium	2.30	0.81	9.72	3.42	0.65	3.77	6.00	15.69	37.62	13.52	0.55	2.50	0.23	3.15	0.05	0.02	3.90
Platinum	1.29	0.09	6.36	1.06	0.03	0.50	2.00	8.19	20.88	58.10	0.06	0.43	0.31	0.33	0.12	0.25	2.62
Chromium	1.14	0.79	5.69	1.29	0.42	6.33	2.30	2.32	1.10	0.08	73.15	1.03	1.41	0.32	2.21	0.43	1.68
Lithium	0.64	0.09	1.50	1.02	0.30	0.69	3.23	4.73	5.08	0.54	0.92	73.86	1.52	2.98	2.65	0.26	1.63
Manganese	0.89	3.52	0.33	0.56	11.86	0.08	0.16	1.99	0.43	0.35	0.71	1.11	66.87	0.50	6.85	3.80	2.07
REE	3.73	0.64	0.54	1.15	0.41	1.09	3.89	5.29	6.09	0.39	0.32	2.19	0.76	70.89	2.49	0.12	1.82
Silicon	1.58	2.38	0.16	0.01	3.20	1.88	0.04	0.14	0.19	0.09	0.88	0.97	6.68	2.13	65.82	13.86	2.14
Vanadium	0.12	3.84	0.22	0.08	6.08	1.17	0.21	0.03	0.12	0.09	0.18	0.26	2.50	0.04	14.91	70.16	1.87
To	2.95	1.34	5.11	3.07	1.97	3.59	4.94	5.15	4.83	1.71	0.92	0.90	2.00	1.16	2.21	1.67	**43.53**
Net	-0.35	-0.16	1.04	-0.39	0.12	0.07	0.91	1.09	0.94	-0.91	-0.76	-0.73	-0.07	-0.66	0.07	-0.19	-

Notes: full sample connectedness. Entry in bold is total connectedness.

Figure B1: Full sample group connectedness measures for returns

(a) Within and cross group connectedness (b) To, From and Net connectedness

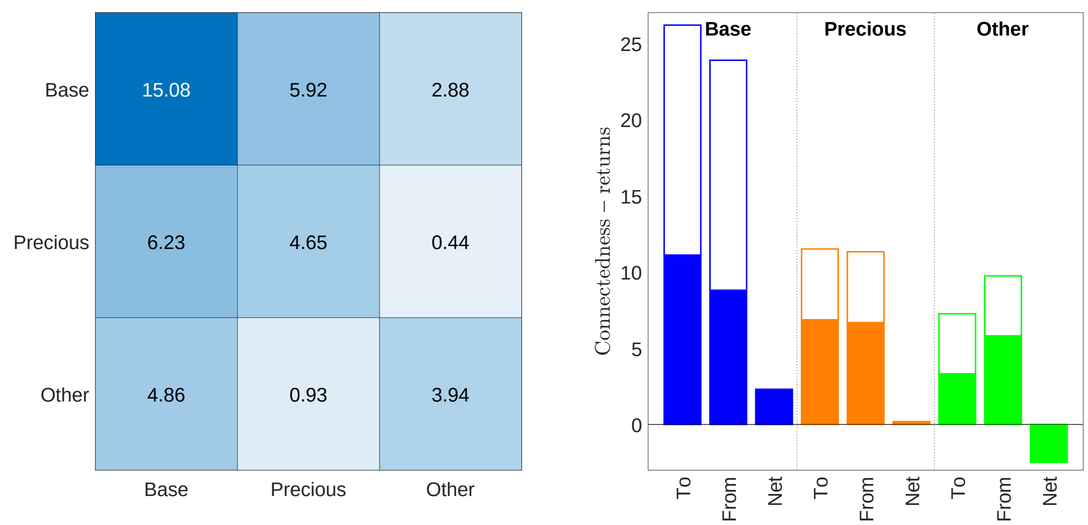

Notes: panel (a) shows within group connectedness along the main diagonal, while off-diagonal elements are cross group connectedness measures. Panel (b) shows the to, from and net connectedness statistics for groups of metals. Colored areas refer to the off-diagonal statistics, whereas the white areas denote statistics comprehending the diagonal elements.

Figure B2: To, From and Net connectedntess – returns

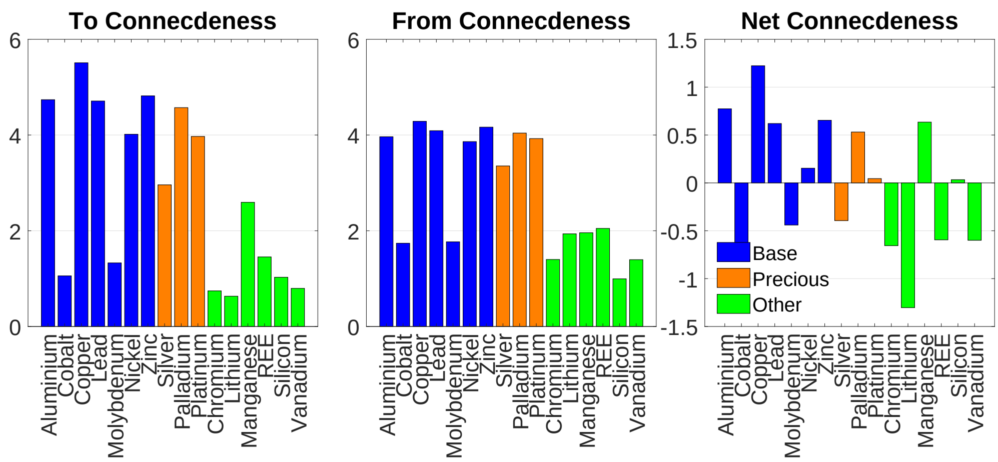

Figure B3: Leads and Lags correlation analysis

(a) Returns connectedness correlation (b) $log\sqrt{RV_t}$ connectedness correlation

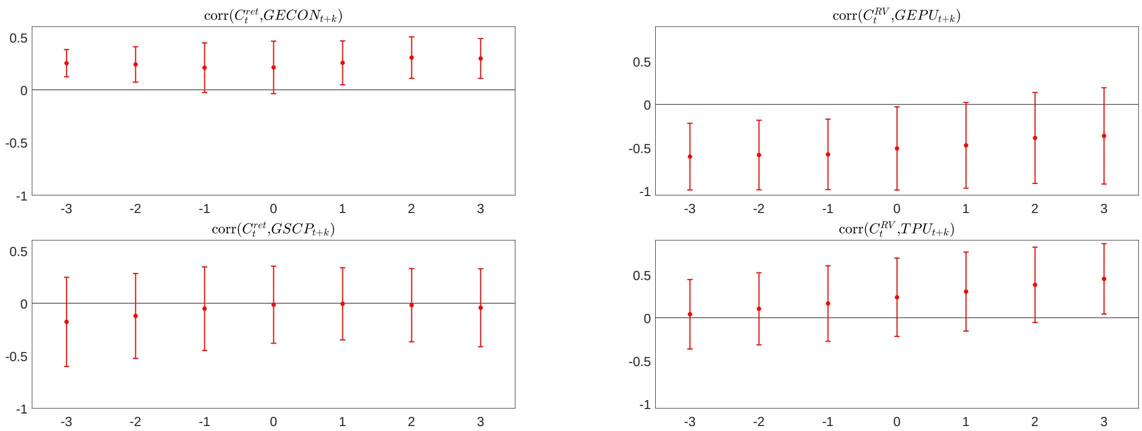

Notes: red bars highlights the correlation coefficient and relative standard deviations for different leads (k up to 3) and lags (k up to -3).

FONDAZIONE ENI ENRICO MATTEI WORKING PAPER SERIES

Our Working Papers are available on the Internet at the following address:
https://www.feem.it/pubblicazioni/feem-working-papers/

"NOTE DI LAVORO" PUBLISHED IN 2023

1. 2023, G. Maccarone, M.A. Marini, O. Tarola, Shop Until You Drop: the Unexpected Effects of Anti-consumerism and Environmentalism
2. 2023, F. Andreolli, C. D'Alpaos, P. Kort, Does P2P trading favor investments in PV-Battery Systems?
3. 2023, M. Buso, C. Dosi, M. Moretto, Dynamic Regulation of Public Franchises with Imperfectly Correlated Demand Shocks
4. 2023, A. Ugolini, J. C. Reboredo, J. Ojea-Ferreiro, Is climate transition risk priced into corporate credit risk? Evidence from credit default swaps
5. 2023, F. Cornacchia, A. G. Martínez-Hernández, M. Bidoia, C. Giupponi, Towards a modelling process for simulating socio-ecosystems with a focus on climate change adaptation
6. 2023. S. Zanini, Water challenges in socio-ecological systems: is human decision-making accounted for in the analysis of climate change adaptation options?
7. 2023, L. Cavalli, C. Boeri, Carbon neutral lifestyles and NDCs: advice and policy perspectives
8. 2023, F. Calamunci, F. Frattini, When Crime Tears Communities Apart: Social Capital and Organised Crime
9. 2023, D. Bazzana, M. Rizzati, E. Ciola, E. Turco, S. Vergalli, Warming the MATRIX: a climate assessment under uncertainty and heterogeneity
10. 2023, A. L. Baraldi, E. Papagni, M. Stimolo, Neutralizing the Tentacles of Organised Crime. Assessment of the Impact of an Anti-Crime Measure on Mafia Violence in Italy
11. 2023, A. Bastianin, C. Casoli, M. Galeotti, The connectedness of Energy Transition Metals

Fondazione Eni Enrico Mattei
Corso Magenta 63, Milano – Italia

Tel. +39 02 403 36934

E-mail: letter@feem.it
www.feem.it

Fondazione Eni Enrico Mattei